# Sensory processing in the Drosophila antennal lobe increases reliability and separability of ensemble odor representations

**Article** *in* Nature Neuroscience · December 2007

DOI: 10.1038/nn1976 · Source: PubMed

CITATIONS
292

READS
219

**5 authors**, including:

Vikas Bhandawat
Drexel University
**28** PUBLICATIONS **1,342** CITATIONS

SEE PROFILE

Rachel I Wilson
Harvard Medical School
**87** PUBLICATIONS **12,312** CITATIONS

SEE PROFILE

Published in final edited form as:
*Nat Neurosci*. 2007 November ; 10(11): 1474–1482. doi:10.1038/nn1976.

# Sensory Processing in the *Drosophila* Antennal Lobe Increases the Reliability and Separability of Ensemble Odor Representations

**Vikas Bhandawat**, **Shawn R. Olsen**[1], **Nathan W. Gouwens**[1], **Michelle L. Schlief**[1], and **Rachel I. Wilson**[*]
Department of Neurobiology, Harvard Medical School, 220 Longwood Ave., Boston MA 02115

## Abstract

Here we describe several fundamental principles of olfactory processing in the *Drosophila* antennal lobe (the analog of the vertebrate olfactory bulb), based on a systematic analysis of input and output spike trains of seven identified glomeruli. Repeated presentations of the same odor elicit more reproducible responses in second-order projection neurons (PNs) than in their presynaptic olfactory receptor neurons (ORNs). PN responses rise and accommodate rapidly, emphasizing odor onset. Furthermore, weak ORN inputs are amplified in the PN layer but strong inputs are not. This nonlinear transformation broadens PN tuning, and produces more uniform distances between odor representations in PN coding space. Additionally, a portion of a PN's odor response profile is not systematically related to its direct ORN inputs, likely reflecting lateral connections between glomeruli. Finally, we show that a linear discriminator classifies odors more accurately using PN spike trains as compared to an equivalent number of ORN spike trains.

Each glomerulus in the olfactory system receives synaptic input from many olfactory receptor neurons (ORNs), all of which express the same odorant receptor gene. Each second-order neuron sends a dendrite into a single glomerulus; thus for each odorant receptor gene there is an identifiable ORN type and a corresponding type of second-order neuron. An odorant typically activates ORNs projecting to multiple glomeruli, and so each odor is represented as a population code across different processing channels[1, 2]. What happens to olfactory signals as they move through these channels? Addressing this question is technically challenging in vertebrates because there are so many glomeruli. In *Drosophila*, the problem is comparatively simpler because the antennal lobe contains only ~50 glomeruli. Each of these glomeruli has a stereotyped position that is identifiable across flies, and almost all have been matched to an identified ORN type[3–6]. For these reasons, it may be easier to discover the basic principles of early olfactory processing in this model organism.

In general, effective information transmission requires that (1) the response evoked by a stimulus should be highly reliable, and (2) the responses evoked by different stimuli should be distinctive. Thus we have focused on two fundamental questions. First, how reproducible is the number of spikes evoked by repeated presentations of the same odor? There has been remarkably little attention paid to the reproducibility of olfactory responses, and the small number of previous studies on this issue have been concerned with the precision of spike timing rather than the reproducibility of spike counts[7, 8]. Response reproducibility is a central issue in sensory processing because the signal-to-noise ratio of a neural response limits the rate of information transmission by that neuron.

[*]Correspondence: rachel_wilson@hms.harvard.edu.
[1]These authors contributed equally to this work.

The second fundamental question concerns the distinctiveness of neural responses to different stimuli. How selective are ORNs, and how does their selectivity compare to that of second-order olfactory neurons? Three studies published more than 20 years ago in vertebrates reached conflicting conclusions on this issue, but it was not feasible for these investigators to directly compare the selectivity of pre- and postsynaptic neurons corresponding to the same glomerulus[9–11]. More recently, three studies made this direct comparison in the *Drosophila* antennal lobe, but again results were conflicting[12–14]. Two of these studies used genetically-encoded sensors which may not report spike trains faithfully due to a limited dynamic range[15, 16]; the third study recorded spike trains directly but compared ORNs and second-order neurons corresponding to only one glomerulus.

Here we aim to resolve these issues with a systematic analysis of the input and output spike trains corresponding to 7 glomeruli in the *Drosophila* antennal lobe (Supplementary Fig. 1 online). Our results demonstrate a major transformation of olfactory representations in this brain region. The most important effects of this transformation are to improve the signal-to-noise ratio of individual spike trains and to distribute odor representations more uniformly in neuronal coding space.

## RESULTS

### Odor responses are more reliable in PNs than in ORNs

The variability of a neuronal response can be quantified as the variability in the number of spikes evoked by a sensory stimulus. In most sensory systems, the spike-count variability of stimulus-evoked responses increases at each successive processing level in a sensory system[17–19]. However, in the *Drosophila* antennal lobe, ~40 ORNs with the same receptive field converge onto ~4 PNs in each glomerulus[20–22]. Thus, by pooling across these inputs, PNs might be able to reduce their response variability. We therefore compared the reliability of odor-evoked spike counts in ORN and PNs.

We presented an odor stimulus in multiple consecutive trials to the same cell (a “block” of trials, Fig. 1a). To quantify spike count reliability across trials, we divided each set of repeated responses into 50-ms windows that overlapped by 25-ms. In each time window, we computed the mean and the standard deviation (SD) of the spike count across repeated responses by the same cell to the same odor. Odors typically evoked more vigorous responses in PNs than in ORNs (Fig. 1a,b; see also Supplementary Fig. 2). So, although the typical SD of PN responses is slightly larger than that of ORN responses (Fig. 1c), PN responses are less variable in proportion to the magnitude of the response (Fig. 1d; $p<10^{-15}$ whether comparing over the entire stimulus period [gray bar] or the 100 ms epoch at the response peak [black bar], Mann-Whitney U-test, $n$=779 ORN responses and 843 PN responses). Thus, individual PNs are more reliable than individual ORNs, which should tend to make their responses more informative.

We also compared the SD of ORN and PN spike counts as a function of the mean spike count for each time window. For all mean spike counts, PNs have a lower SD than ORNs (Fig. 1e). Furthermore, the SD is not strongly dependent on the mean, and so stronger responses have a lower CV. Because PN responses are on average stronger than ORN responses (Fig. 1b), this also tends to make PNs more reliable than ORNs.

### PNs preferentially transmit rising phase of ORN signals

ORN responses typically do not peak until 100–300 ms after odor onset[21]. This is probably because spiking is coupled to odorant receptor activation by the G-protein-mediated generation of second messengers. However, odors can trigger rapid behavioral responses in flies, with a total latency from stimulus to motor reaction of less than 300 ms[23]. This suggests that neurons

in the brain are preferentially tuned to detect the rising phase of ORN signals, rather than the response peak. This motivated us to compare the onset kinetics of odor responses in synaptically connected ORNs and PNs.

Comparing peri-stimulus time histograms averaged across all odor responses in all cells, we noted that PN responses rise more rapidly than ORN responses (Fig. 2a). Furthermore, PN responses begin to decay while ORN responses are still growing. This is also clear in most direct comparisons between synaptically connected ORNs and PNs responding to the same odor (Fig. 2b,c and Fig. 1a). Overall, PN responses peak significantly faster than ORN responses (Fig. 2d, $p<10^{-7}$, paired t-test, $n$=69 odor/glomerulus combinations), and the time to half-decay of the response is shorter for PNs than for their presynaptic ORNs (Fig. 2e, $p<10^{-5}$, paired t-test). Taken together, faster rise and faster decay mean that more excitatory drive to third-order neurons occurs within an early epoch of the odor response (Fig. 2f, $p<10^{-11}$, paired t-test). Thus PNs act as high-pass filters which preferentially signal the rising phase of the ORN response.

Because PN responses accommodate rapidly, we have chosen to quantify response magnitudes in PNs by measuring average firing rates during an early epoch of the response (a 100-ms time window beginning 100 ms after odor onset, see black bar in Fig. 1b). Because a fruit fly can respond rapidly after encountering an odor, this early epoch should be particularly informative to downstream neurons. Throughout this study, we have also quantified PN responses in a different way: following other investigators[21, 24], we have measured average spike rates over the entire 500-ms stimulus period. The major conclusions of this study are the same for both of these response metrics.

## ORNs and PNs differ in selectivity and odor preferences

Now setting aside the issues of trial-to-trial reliability and response kinetics, we examined the average response magnitudes for each cell type to our odor stimuli. How does the response profile of each PN type compare to the response profile of its corresponding ORNs? We began by asking simply if these responses are linearly correlated. For each glomerulus we found a statistically significant correlation between the ORN and PN response profile ($p<0.05$ for all 7 glomerular comparisons, Pearson's correlation, Supplementary Table 1), but $r^2$ values are only in the range of 0.26–0.81. This means that a linear scaling of ORN responses only explains 26–81% of the odor-dependent variance in PN responses.

Two features of PN odor responses diminish this linear correlation. First, for each glomerulus, PNs are less selective than their presynaptic ORNs ($p<0.05$, Wilcoxon signed rank test, Fig. 3b, similar results in Supplementary Fig. 3). To test the generality of this result, we also compared ORN and PN selectivity for glomerulus DM4 at three different odor concentrations. Like our standard concentration (1:1,000 dilution), weaker stimuli (1:10,000 and 1:100,000 dilutions) produce PN response profiles that are less selective than the corresponding ORN response profiles (Fig. 4). Other investigators using identical stimulus conditions have shown that ORN responses are very sparse at the 1:100,000 dilution, indicating that this concentration is near the bottom of this system's dynamic range[21, 22, 24, 25]. These results show that broad PN tuning is not a phenomenon limited to high odor concentrations.

Another factor that diminishes this linear correlation is that the rank order of odor preferences differs for ORNs and PNs. For example, whereas ethyl butyrate is the 3$^{rd}$-ranked odor of DL1 PNs, it is only ranked 16$^{th}$ among the odor responses of DL1 ORNs (Fig. 3a). Some of this difference is merely due to errors in estimating each average response profile on the basis of a limited sample of individual experiments. However, sampling error cannot completely account for this result. This can be shown by pairing an individual ORN with a corresponding individual PN and computing the correlation between their odor ranks, and then comparing the

distribution of these correlations with the correlations obtained from ORN/ORN or PN/PN pairings. Because we were not able to test every odor in every experiment, we assembled many simulated response profiles by drawing randomly from a normal distribution defined by the mean and standard deviation of each average response profile (illustrated in Fig. 5a, see also Supplementary Methods). The median correlation between ORN and PN ranks was only 0.47, which is substantially lower than the correlation between ORNs of the same type or between PNs of the same type (0.65 and 0.61 respectively, Fig. 5). The simplest explanation for this result is that a PN's odor preferences are significantly influenced by lateral connections between glomeruli[26, 27].

## A nonlinear transformation function for each glomerulus

Clearly, the output of a glomerulus is not a simple a linear scaling of its inputs. Furthermore, because ORNs and PNs differ in their ranked odor preferences, no monotonic function can describe the relationship between the ORN and PN response profile for a glomerulus. We therefore asked if there is any systematic relationship between ORN and PN responses. For each glomerulus, we plotted PN responses to each odor as a function of ORN responses to the same odor (Fig. 6a). This revealed a consistent transformation function for each glomerulus, albeit with some scatter. These functions have a similar shape for most glomeruli: they initially slope steeply, meaning that the gain of the transformation function is high for weak inputs. As ORN input levels increase these curves flatten, meaning that the gain of the transformation function decreases. (This is true for all glomeruli we tested except DL1.) In sum, these plots show that PNs inherit much of their tuning from their presynaptic ORNs, but the transformation is highly nonlinear.

This type of transformation function may be useful because it makes better use of a PN's available response range. This is illustrated by projecting the points in each plot onto both the *x*- and *y*-axes (Fig. 6a, green and magenta symbols). ORNs are not using all parts of their dynamic range with equal frequency, since most of our stimuli elicit responses confined to a narrow range of firing rates. However, two odors that elicit similarly weak levels of activity in an ORN (green) can elicit quite different levels of activity in a postsynaptic PN (magenta), because each glomerular transformation function shows high gain at low ORN input levels. This tends to distribute the responses to these stimuli more uniformly throughout the response range of each PN.

This type of sensory transformation has been termed "histogram equalization"[28] because it produces a flatter histogram of response intensities. To examine whether this is occurring across the entire population of cells in our data set, we plotted the distribution of response intensities for ORNs and PNs, accumulated across all odors and all glomeruli (Fig. 6b). The ORN response histogram shows a large peak at low response intensities, and a long flat tail covering the rest of the ORN dynamic range. The PN response histogram, by contrast, is much flatter, meaning that all available response intensities are used with more uniform frequency. In this sense, PNs encode our odor stimuli more efficiently than ORNs do.

Although there is clearly an overall relationship between ORN and PN responses for each glomerulus, it is also important to note that these functions do not predict PN odor responses completely. Because ORNs and PNs differ in their ranked odor preferences, no monotonic function will account for all this data.

## Odor representations in multi-glomerular coding space

Third-order neurons receive convergent input from multiple PN types[29–32]. It is therefore important to examine odor representations in multi-glomerular coding space. In the simplest case, histogram equalization in one dimension should also produce a more uniform distribution

of odors in multiple dimensions. In order to visualize odor representations in 7-dimensional space, we reduced the dimensionality of this space by performing principal components analysis (PCA). The first two principal components define the two-dimensional projection that maximizes the variance of the data. In this projection, most odors are still clustered near the origin of ORN space, with only a few odors located far from this cluster (Fig. 7a). In the equivalent PN space, odors fill the available coding space more uniformly (Fig. 7b).

Thus, as a result of the ORN-to-PN transformation, odor representations are distributed more efficiently in multi-glomerular coding space. In concrete terms, the ensemble patterns of spiking activity elicited by any two odors become more different. We quantified this by measuring Euclidean distances between odors in 7-dimensional space for all possible pair-wise combinations of odors ([18 choose 2]=153 pairs). During the early epoch of odor responses (black bar), distances are significantly larger in PN space as compared to ORN space ($p<0.0001$, paired t-test, $n=153$). Moreover, the distribution of distances is narrower for PNs than for ORNs over the entire stimulus period (note inter-quartile range in Fig. 7c versus 7d). This means that odors are distributed more uniformly in PN coding space. Some odor distances decrease, but others increase.

Is the separation of odors in multi-dimensional space larger or smaller than we would predict simply on the basis of independent odor separation in each one-dimensional coding channel? The answer depends on the degree of correlation between different glomeruli. Lateral connections clearly shape PN odor responses (Fig. 5 and refs. [26, 27]); if these connections increased correlations between different PN types, this would decrease inter-odor distances in multi-dimensional space. To address this issue, we constructed a simulated data set that preserves the distribution of response magnitudes for each glomerular cell type, but breaks any dependencies between odor responses in different glomeruli. We achieved this by independently shuffling the odor labels on each glomerular response profile. We then measured inter-odor distances in 7-dimensional space for all possible pair-wise combinations of odors. When we repeated this simulation many times, the range of distances we obtained was indistinguishable from the distances we measured in our real data set (Fig. 7c,d). This means the separation between ensemble odor representations is roughly what we would predict based simply on histogram equalization in each glomerulus individually.

## Correlations between cell types and odors

We have seen that PNs use all portions of their dynamic range with approximately equal frequency, and in this sense encode odors more efficiently than ORNs do[28]. However, the term “efficient coding” has also been applied to the idea that the responses of different neurons should be maximally independent from each other[33]. We measured the independence of different glomerular coding channels by computing the percentage of the variance in the ensemble odor responses that is captured by each of the 7 principal components (PCs) of the 7-dimensional ORN or PN coding space. If all 7 cell types were completely correlated, then the first PC would account for 100% of the variance in the data. In other words, all the data would lie along a single line in multi-dimensional space. Conversely, if all cell types were perfectly decorrelated, and if the data was distributed according to a multi-dimensional Gaussian, then each PC would account for an equal amount of the total variance (100% ÷ 7 = ~14%). (Even in this case, we would need a very large odor set to discern this perfect decorrelation.)

The PCs of our data set fall between these hypothetical extremes (Fig. 8a). In part, this simply reflects the limited size of our odor set and the non-Gaussian distribution of the ORN response histograms (see Fig. 6b). We demonstrated this by independently and randomly shuffling the odor labels on each of the 7 ORN response profiles and recomputing the PCs of this simulated data set. These simulations always produced a first PC that accounted for a disproportionately

large share of the variance (usually 30–40%, Fig. 8a). However, the PCs of the real (non-shuffled) data set are even more skewed, with the first PC accounting for 54% of the variance. This means that ORNs in different glomeruli have odor preferences that are more highly correlated than we would expect based simply on the distribution of response magnitudes in each glomerular channel.

Similarly, about half the variance in the PN data is captured by the first PC (51%, Fig. 8b). This is mainly due to the limited size of our odor set and the non-Gaussian distribution of the PN response histograms, since shuffling odor labels on each PN response profile always produced a skewed distribution of PC contributions (Fig. 8b). Because real PN data produced a distribution that was even more skewed than the simulated data, PNs (like ORNs) are more correlated than we would expect based simply on the distribution of response magnitudes for each PN type.

In sum, sensory processing in the *Drosophila* antennal lobe does not change the degree of independence between different glomerular coding channels. The conclusions of this analysis are similar regardless of whether we measure spike rates around the response peak (Fig. 8), or over the entire stimulus period (Supplementary Fig. 6).

## PN odor responses are more separable than ORN responses

Increased PN reliability and more uniform odor distances in PN coding space should mean that odors are more discriminable on the basis of PN spike trains as compared to an equivalent number of ORN spike trains. We tested this prediction by measuring the ability of an algorithm to identify the odor stimulus based on the ensemble neural response elicited by that odor. Because our data come from single (not multi-unit) ORN and PN recordings, we simulated "multi-unit" responses by assembling data from different glomerular classes. Each simulated data set comprised 90 multi-unit responses (18 odors, 5 spike trains per odor per cell). We performed linear discriminant analysis to identify the linear combinations of input variables that best separated all 18 odor response clusters from each other. To evaluate the quality of these discriminations, we held out one multi-unit odor response from the data set, trained the algorithm with the remaining 89, and predicted the odor corresponding to the one held-out response. The predicted odor was then compared to the actual odor. We repeated this analysis with many independently assembled multi-unit responses at each time point in the odor response.

Prior to odor onset, the prediction success rate hovers near chance (Fig. 9a). (The success rate is slightly above chance because different cells had somewhat different spontaneous firing rates, and spontaneous firing rates sometimes drifted during an experiment; thus, spontaneous firing rates were slightly "predictive" of the odor because successive trials with an odor were presented consecutively rather than interleaved). After odor stimulus onset, success rates rise rapidly. As expected, including more glomerular classes in the data set produces higher success rates (Fig. 9b). Because success rates using PN data hit a ceiling at 100% for some classifications using data from >3 glomeruli, this procedure underestimates the difference in discriminability between ORN and PN responses. Nevertheless, success rates are significantly higher for PN data than for ORN data for all conditions in Fig. 9b ($p<0.005$, Mann-Whitney U-tests, $n=20$ runs of the classification procedure for ORNs and PNs for each condition). This demonstrates that a linear discriminator can classify odors more accurately with responses from several PNs than with responses from the same number of ORNs.

# DISCUSSION

## An improved signal-to-noise ratio

Studies in other systems have implied that the variability of stimulus-evoked spike counts almost always increases at successively higher levels of sensory processing[34]. For example, visual responses of higher cortical neurons are often very noisy[17], in contrast to the reliability of retinal ganglion cells[35]. A direct comparison of responses evoked by identical stimuli in the retina, thalamus, and visual cortex has confirmed that spike-count reliability decreases at each successively higher level of the visual stream[18]. This is despite the fact that a simple cell in primary visual cortex pools signals from ~30 thalamic neurons[36], which ought to improve its reliability. Similarly, a direct comparison of spike trains at successive levels of an insect auditory circuit has found that noise increases at successively higher levels[19]. Our results show a different trend: spike counts in individual PNs are significantly more consistent than spike counts in individual ORNs. This is partly because PNs tend to fire more vigorously than their presynaptic ORNs in response to the same stimulus, and stronger responses are more reliable for both ORNs and PNs. This may imply an increasingly deterministic control of spike timing at high firing rates due to intrinsic refractoriness[37]. However, even at the same firing rates, PN responses are more reliable than ORN responses. This may reflect the benefits of pooling: each PN is postsynaptic to many ORNs, and all these ORNs respond similarly to odors[21, 22, 38]. If noise is uncorrelated across ORNs, then pooling these inputs should tend to improve the reliability of PN responses.

On balance, the improvement in reliability is smaller than one might predict. Each glomerulus corresponds to ~40 ORNs and ~4 PNs; this means the average PN pools inputs from 10 to 40 ORNs (depending on whether each ORN contacts all PNs in a glomerulus). Since pooling $N$ ORN inputs should decrease the variability of the pooled average by $\sqrt{N}$, we would expect the coefficient of variation to improve by $\sqrt{10}$ to $\sqrt{40}$. The effect we describe is on the low end of this range, suggesting that each ORN contacts only a single PN, or that PNs receive additional noise from other neuronal sources.

## High-pass filtering of olfactory signals

Our results show that PNs can be extremely sensitive to small differences between weak levels of ORN input. Even a small increase in ORN spike rate above baseline can produce a robust response in postsynaptic PNs. As a result, PN responses rise rapidly even when ORN responses build slowly. This is particularly useful because the onset kinetics of ORNs are intrinsically limited by the speed of signal transduction cascades linking odorant receptor activation to spike initiation. PN responses then rapidly decline while ORN spike rates are still rising. This means that PNs act as high-pass filters, transmitting the rising phase of ORN responses preferentially over the tonic component of ORN responses. This rapid accommodation might be due to any of several mechanisms, including for example short-term synaptic depression at the ORN-to-PN synapse.

Taken together, a faster rise and a faster decay should sharpen the estimate of odor arrival time by downstream neurons. For a fly in flight, this should translate into an improved estimate of odor plume location. Notably, *Drosophila* can turn in flight less than 300 ms after encountering an odor plume[23]. A similar phenomenon operates in the visual system, where sluggish photoreceptor responses trigger speedy depolarizations in downstream neurons[39] and ultimately rapid behavioral responses to visual stimuli.

We note that *Drosophila* PN responses differ from the responses of locust PNs, which typically show more complex temporal patterning[29, 40, 41]. Locust PNs also show a higher average level of maintained activity throughout the odor response (relative to response peak) and also often

display excitatory responses to odor offset[41]. By contrast, *Drosophila* PNs accommodate rapidly and typically do not burst after stimulus offset (but for some exceptions see Supplementary Fig. 2f).

## A nonlinear transformation increases coding efficiency

A major finding of this study is that although PNs inherit a substantial portion of their odor tuning from their presynaptic ORNs, this relationship is highly nonlinear. This nonlinearity disproportionately amplifies small differences between weak levels of ORN input. By contrast, small differences between strong ORN inputs are not amplified to the same degree. Most ORN odor responses cluster in the weak end of the ORN's dynamic range. As a result of this nonlinear transformation, PNs use their dynamic range more uniformly than ORNs do. If all portions of a neuron's dynamic range are used with equal frequency, the carrying capacity of that information channel is maximized because the entropy of the neuron's response is maximized. This tends to protect signals from contamination by noise added at later stages in the processing channel[42]. This has long been recognized to be a useful computation in sensory processing[28]. If broader tuning curves might be useful, why has evolution not simply produced broadly tuned ORNs? ORN responses are directly linked to the way odorant receptor proteins interact with odor molecules; therefore broadening ORN tuning might require changing the biophysics of odorant receptors in ways that are unfavorable for other reasons.

Broad PN tuning may seem counter-intuitive: we tend to think of higher-order neurons as being more selective than their presynaptic inputs. These expectations are founded in part on the paradigm of visual processing, where successive layers of higher-order neurons are increasingly specialized to represent complex conjunctions of visual features. However, there is also a huge expansion in the number of higher-order neurons devoted to representing complex visual features as compared to the number of retinal ganglion cells. Thus the dimensionality of higher visual representations is increasingly large, so these brain regions can afford to code information increasingly sparsely as ensembles of narrowly-tuned neurons. By contrast, in early olfactory processing, the dimensionality of the second-order representation is the same as the dimensionality of the first-order representation. Thus, total coding space cannot increase (unless time is used as an additional coding dimension[43]).

It is important to note that, in a truly efficient coding scheme, neurons should efficiently encode natural stimulus distributions, not arbitrary stimulus distributions[28]. Although our odor set is chemically diverse and relatively large, it may not be representative of the odors a wild fly would encounter. In the future, it would be interesting to learn whether the principles of olfactory processing we describe here also apply to a more naturalistic distribution of odor stimuli.

Another caveat is that we have not sampled all antennal lobe glomeruli. However, because most of the glomeruli in our data set showed a similar nonlinear transformation function, our conclusions likely generalize to many glomeruli outside our data set. An interesting special case is glomerulus DA1, which was not included in our data set. ORNs projecting to this glomerulus respond weakly but highly selectively to a *Drosophila* pheromone. Their postsynaptic PNs are also highly selective for this odor, but respond much more robustly[44]. Thus, this processing channel exhibits amplification without a change in response selectivity.

## Ensemble odor responses

Extending our analysis from one glomerular channel to multi-glomerular ensembles, we found that odors are more uniformly separated in ensemble PN coding space as compared to ensemble ORN coding space. This separation is approximately what we would expect based on the increased separation between odors within each glomerular coding channel. We demonstrated

this using a simulation that made the odor preferences of each glomerulus independent from each other, while preserving the characteristic response magnitudes of each cell type.

We also found that sensory processing in the antennal lobe does not substantially alter the independence of different glomerular coding channels. The degree of correlation between different PN types is similar to the degree of correlation between different ORN types. Interestingly, ORNs have more correlated odor preferences than we would expect simply on the basis of their tuning breadth and the size of our odor set. We also obtained the same result by re-analyzing a large published data set[24] comprising 24 *Drosophila* ORN types and 110 odors (result not shown). This result may be due to the common evolutionary origin of different *Drosophila* odorant receptors in gene duplication events[45]. In addition, some odors are intrinsically more volatile than others, which will tend to produce similarities in the odor preferences of different glomeruli. Like ORNs, PNs are also somewhat more correlated than we would expect based on their tuning breadth and the size of our odor set. This may simply reflect correlations inherited from ORNs.

## The role of lateral connections between glomeruli

Glomeruli in the *Drosophila* antennal lobe are connected by both GABAergic interneurons[20, 46] and cholinergic interneurons[26, 27]. What is the role of these connections in the transformations we have described?

We have noted that the rank order of PN odor preferences is different from the order of ORN odor preferences. We show that this difference is too large to be explained by the uncertainty in our estimates of each average odor response profile (Fig. 5). Therefore, some of this difference is probably caused by lateral inter-glomerular connections, because lateral inputs would have an odor tuning that reflects the odor preferences of ORNs presynaptic to other glomeruli. In principle, either inhibitory or excitatory lateral connections could cause this phenomenon. The computational significance of this phenomenon is not clear, since it does not seem to decorrelate the responses of PNs in different glomeruli (Fig. 8).

It is easy to see how lateral connections could cause scatter around each glomerular transformation function. However, lateral connections may also play an important role in determining the underlying shape of these transformation functions. For example, all of these functions have a *y*-intercept >0 (Fig. 6). This reflects the tendency of PNs to respond weakly to an odor even when their presynaptic ORNs are not responding at all. Lateral excitatory connections are strong enough to trigger these responses[26, 27]. Moreover, lateral inhibition could act on ORN axon terminals to govern the probability of neurotransmitter release, and thereby contribute to a nonlinear relationship between pre- and postsynaptic activity. At the analogous synapse in the olfactory bulb, ORN-to-mitral cell synapses show strong frequency-dependent short-term plasticity that is modulated by presynaptic inhibition via GABAergic local neurons[47]. Thus, we should not assume that the systematic relationships in Fig. 6 are purely intrinsic to each glomerulus. More mechanistic experiments will be required to disentangle the role of intra- versus inter-glomerular mechanisms in shaping these transformation functions.

## Odor discriminability

We have shown that a linear discriminator can identify odors more accurately on the basis of PN spike trains than on the basis of an equivalent number of ORN spike trains. This is likely due to both the increased distances between odors in PN space, and the improved signal-to-noise ratio among PNs. It is important to point out that linear discriminant analysis is not meant to emulate a biologically plausible downstream neuron, and that real third-order neurons will be subject to more constraints than our algorithm is. Also, this is not an optimal decoder, and

so its performance may not reflect the total amount of information in the responses it decodes. Finally, the total amount of information in the entire PN ensemble cannot, of course, exceed the total amount of information in the entire ORN ensemble. What we have shown here is that the information in a limited subset of the PN ensemble is more useful for a linear decoder than the information in an equivalent number of ORNs. This is an important demonstration of the potential functional consequence of increased PN reliability, combined with increased inter-odor distances in PN coding space.

In conclusion, we have described two fundamental tasks accomplished by the first stage of the olfactory processing stream. On a neuron-to-neuron basis, our comparisons show that signal reproducibility is increased, and distinctions between the responses to different stimuli are enhanced. The details of odor processing in the vertebrate olfactory bulb could be very different, especially because the number of glomeruli in vertebrates is much larger. Nevertheless, most organisms share a common olfactory processing architecture, suggesting that some of the basic principles we have demonstrated in flies may also apply to vertebrates.

## METHODS

### Fly stocks

Flies were reared at room temperature on conventional cornmeal agar. All experiments were performed on adult female flies 2–7 days post-eclosion. Supplementary Table 4 lists genotypes for all experiments. See Supplementary Methods for stock origins.

### ORN recordings

Flies were immobilized in the trimmed end of a plastic pipette tip under a 50× air objective mounted on a Olympus BX51WI microscope. A reference electrode filled with saline was inserted into the eye, and a sharp saline-filled glass capillary (tip diameter < 1μm) was inserted into a sensillum. Recordings were obtained with an A-M Systems Model 2400 amplifier, low-pass filtered at 2 kHz, and digitized at 10 kHz. ORN spikes were detected using routines in IgorPro (Wavemetrics). See Supplementary Methods for details.

### PN recordings

Whole-cell recordings from PN somata were performed *in vivo* as previously described[46]. One neuron was recorded per brain and the morphology of each cell was visualized *post hoc* with biocytin-streptavidin and nc82 histochemistry as described previously[46], except that in the secondary incubation we used 1:250 goat anti-mouse:AlexaFluor633 and 1:1000 streptavidin:AlexaFluor568 (Molecular Probes). See Supplementary Methods for details.

### Olfactory stimulation

We chose a panel of 18 odors to maximize the chemical diversity of our stimuli, and to maximize overlap with odors used in other studies of the same ORNs[24, 22]. For all experiments (except in Fig. 4), odors were diluted 1:100 v/v in paraffin oil (J.T. Baker, VWR #JTS894), except 3-methylthio-1-propanol, which was diluted 1:100 v/v in water, and 4-methyl phenol, which was diluted 1:100 w/v in water. In Fig. 4, odors were diluted 1:100, 1:1000, or 1:10,000 in paraffin oil. See Supplementary Methods for details.

### Data analysis

See Supplementary Methods for data analysis details.

## Supplementary Material

Refer to Web version on PubMed Central for supplementary material.

## Acknowledgments

We thank K. Ito, L. Luo, L.B. Vosshall, and L.M. Stevens for gifts of fly stocks. We benefited from helpful conversations with S.A. Baccus, V. Jayaraman, H. Kazama, A.W. Liu, J.H.R. Maunsell, O. Mazor, M. Meister, R.C. Reid, H. Sompolinsky, G.C. Turner, and Y. Zhou. This work was funded by a grant from the NIH (1R01DC008174-01), a Pew Scholar Award, a McKnight Scholar Award, a Smith Family Foundation New Investigators Award, and an Armenise-Harvard Junior Faculty Award (to R.I.W.). S.R.O is supported by a NSF Predoctoral Fellowship. N.W.G. is supported by a HHMI Predoctoral Fellowship. M.L.S. is supported by a NIH Postdoctoral Fellowship (1F32DC008741-01A1).

## References

1. Bargmann CI. Comparative chemosensation from receptors to ecology. Nature 2006;444:295–301. [PubMed: 17108953]
2. Mombaerts P. Genes and ligands for odorant, vomeronasal and taste receptors. Nat Rev Neurosci 2004;5:263–78. [PubMed: 15034552]
3. Laissue PP, et al. Three-dimensional reconstruction of the antennal lobe in Drosophila melanogaster. J Comp Neurol 1999;405:543–52. [PubMed: 10098944]
4. Hallem EA, Carlson JR. The odor coding system of Drosophila. Trends Genet 2004;20:453–9. [PubMed: 15313555]
5. Couto A, Alenius M, Dickson BJ. Molecular, anatomical, and functional organization of the Drosophila olfactory system. Curr Biol 2005;15:1535–47. [PubMed: 16139208]
6. Fishilevich E, Vosshall LB. Genetic and functional subdivision of the Drosophila antennal lobe. Curr Biol 2005;15:1548–53. [PubMed: 16139209]
7. Stopfer M, Laurent G. Short-term memory in olfactory network dynamics. Nature 1999;402:664–8. [PubMed: 10604472]
8. Bazhenov M, Stopfer M, Sejnowski TJ, Laurent G. Fast odor learning improves reliability of odor responses in the locust antennal lobe. Neuron 2005;46:483–92. [PubMed: 15882647]
9. Derby CD, Ache BW. Quality coding of a complex odorant in an invertebrate. J Neurophysiol 1984;51:906–24. [PubMed: 6726317]
10. Mathews DF. Response patterns of single neurons in the tortoise olfactory epithelium and olfactory bulb. J Gen Physiol 1972;60:166–80. [PubMed: 5049077]
11. Duchamp A. Electrophysiological responses of olfactory bulb interneurons to odor stimuli in the frog. A comparison with receptor cells. Chem Senses 1982;7:191–210.
12. Ng M, et al. Transmission of olfactory information between three populations of neurons in the antennal lobe of the fly. Neuron 2002;36:463–74. [PubMed: 12408848]
13. Wang JW, Wong AM, Flores J, Vosshall LB, Axel R. Two-photon calcium imaging reveals an odor-evoked map of activity in the fly brain. Cell 2003;112:271–82. [PubMed: 12553914]
14. Wilson RI, Turner GC, Laurent G. Transformation of olfactory representations in the Drosophila antennal lobe. Science 2004;303:366–70. [PubMed: 14684826]
15. Pologruto TA, Yasuda R, Svoboda K. Monitoring neural activity and [Ca2+] with genetically encoded Ca2+ indicators. J Neurosci 2004;24:9572–9. [PubMed: 15509744]
16. Sankaranarayanan S, Ryan TA. Real-time measurements of vesicle-SNARE recycling in synapses of the central nervous system. Nat Cell Biol 2000;2:197–204. [PubMed: 10783237]
17. Shadlen MN, Newsome WT. The variable discharge of cortical neurons: implications for connectivity, computation, and information coding. J Neurosci 1998;18:3870–96. [PubMed: 9570816]
18. Kara P, Reinagel P, Reid RC. Low response variability in simultaneously recorded retinal, thalamic, and cortical neurons. Neuron 2000;27:635–46. [PubMed: 11055444]
19. Vogel A, Hennig RM, Ronacher B. Increase of neuronal response variability at higher processing levels as revealed by simultaneous recordings. J Neurophysiol 2005;93:3548–59. [PubMed: 15716366]

20. Stocker RF, Heimbeck G, Gendre N, de Belle JS. Neuroblast ablation in Drosophila P[GAL4] lines reveals origins of olfactory interneurons. J Neurobiol 1997;32:443–56. [PubMed: 9110257]
21. de Bruyne M, Clyne PJ, Carlson JR. Odor coding in a model olfactory organ: the Drosophila maxillary palp. J Neurosci 1999;19:4520–32. [PubMed: 10341252]
22. de Bruyne M, Foster K, Carlson JR. Odor coding in the Drosophila antenna. Neuron 2001;30:537–52. [PubMed: 11395013]
23. Budick SA, Dickinson MH. Free-flight responses of Drosophila melanogaster to attractive odors. J Exp Biol 2006;209:3001–17. [PubMed: 16857884]
24. Hallem EA, Carlson JR. Coding of odors by a receptor repertoire. Cell 2006;125:143–60. [PubMed: 16615896]
25. Hallem EA, Ho MG, Carlson JR. The molecular basis of odor coding in the Drosophila antenna. Cell 2004;117:965–79. [PubMed: 15210116]
26. Olsen SR, Bhandawat V, Wilson RI. Excitatory interactions between olfactory processing channels in the Drosophila antennal lobe. Neuron 2007;54:89–103. [PubMed: 17408580]
27. Shang Y, Claridge-Chang A, Sjulson L, Pypaert M, Miesenbock G. Excitatory local circuits and their implications for olfactory processing in the fly antennal lobe. Cell 2007;128:601–12. [PubMed: 17289577]
28. Laughlin S. A simple coding procedure enhances a neuron's information capacity. Z Naturforsch [C] 1981;36:910–2.
29. Perez-Orive J, et al. Oscillations and sparsening of odor representations in the mushroom body. Science 2002;297:359–65. [PubMed: 12130775]
30. Marin EC, Jefferis GS, Komiyama T, Zhu H, Luo L. Representation of the glomerular olfactory map in the Drosophila brain. Cell 2002;109:243–55. [PubMed: 12007410]
31. Wong AM, Wang JW, Axel R. Spatial representation of the glomerular map in the Drosophila protocerebrum. Cell 2002;109:229–41. [PubMed: 12007409]
32. Tanaka NK, Awasaki T, Shimada T, Ito K. Integration of chemosensory pathways in the Drosophila second-order olfactory centers. Curr Biol 2004;14:449–457. [PubMed: 15043809]
33. Simoncelli EP. Vision and the statistics of the visual environment. Curr Opin Neurobiol 2003;13:144–9. [PubMed: 12744966]
34. Shadlen MN, Newsome WT. Noise, neural codes and cortical organization. Curr Opin Neurobiol 1994;4:569–79. [PubMed: 7812147]
35. Berry MJ, Warland DK, Meister M. The structure and precision of retinal spike trains. Proc Natl Acad Sci U S A 1997;94:5411–6. [PubMed: 9144251]
36. Alonso JM, Usrey WM, Reid RC. Rules of connectivity between geniculate cells and simple cells in cat primary visual cortex. J Neurosci 2001;21:4002–15. [PubMed: 11356887]
37. Berry MJ 2nd, Meister M. Refractoriness and neural precision. J Neurosci 1998;18:2200–11. [PubMed: 9482804]
38. Shanbhag SR, Muller B, Steinbrecht RA. Atlas of olfactory organs of Drosophila melanogaster. 1 Types, external organization, innervation, and distribution of olfactory sensilla. Int J Insect Morphol Embryol 1999;28:377–397.
39. Armstrong-Gold CE, Rieke F. Bandpass filtering at the rod to second-order cell synapse in salamander (Ambystoma tigrinum) retina. J Neurosci 2003;23:3796–806. [PubMed: 12736350]
40. Stopfer M, Jayaraman V, Laurent G. Intensity versus identity coding in an olfactory system. Neuron 2003;39:991–1004. [PubMed: 12971898]
41. Mazor O, Laurent G. Transient dynamics vs. fixed points in odor representations by locust antennal lobe projection neurons. Neuron 2005;48:661–73. [PubMed: 16301181]
42. Laughlin SB, Howard J, Blakeslee B. Synaptic limitations to contrast coding in the retina of the blowfly Calliphora. Proc R Soc Lond B Biol Sci 1987;231:437–67. [PubMed: 2892202]
43. Laurent G. Olfactory network dynamics and the coding of multidimensional signals. Nat Rev Neurosci 2002;3:884–95. [PubMed: 12415296]
44. Schlief ML, Wilson RI. Olfactory processing and behavior downstream from highly selective receptor neurons. Nat Neurosci 2007;10:623–30. [PubMed: 17417635]

45. Nozawa M, Nei M. Evolutionary dynamics of olfactory receptor genes in Drosophila species. Proc Natl Acad Sci U S A 2007;104:7122–7. [PubMed: 17438280]

46. Wilson RI, Laurent G. Role of GABAergic inhibition in shaping odor-evoked spatiotemporal patterns in the Drosophila antennal lobe. J Neurosci 2005;25:9069–79. [PubMed: 16207866]

47. Wachowiak M, et al. Inhibition of olfactory receptor neuron input to olfactory bulb glomeruli mediated by suppression of presynaptic calcium influx. J Neurophysiol 2005;94:2700–12. [PubMed: 15917320]

48. Vinje WE, Gallant JL. Sparse coding and decorrelation in primary visual cortex during natural vision. Science 2000;287:1273–6. [PubMed: 10678835]

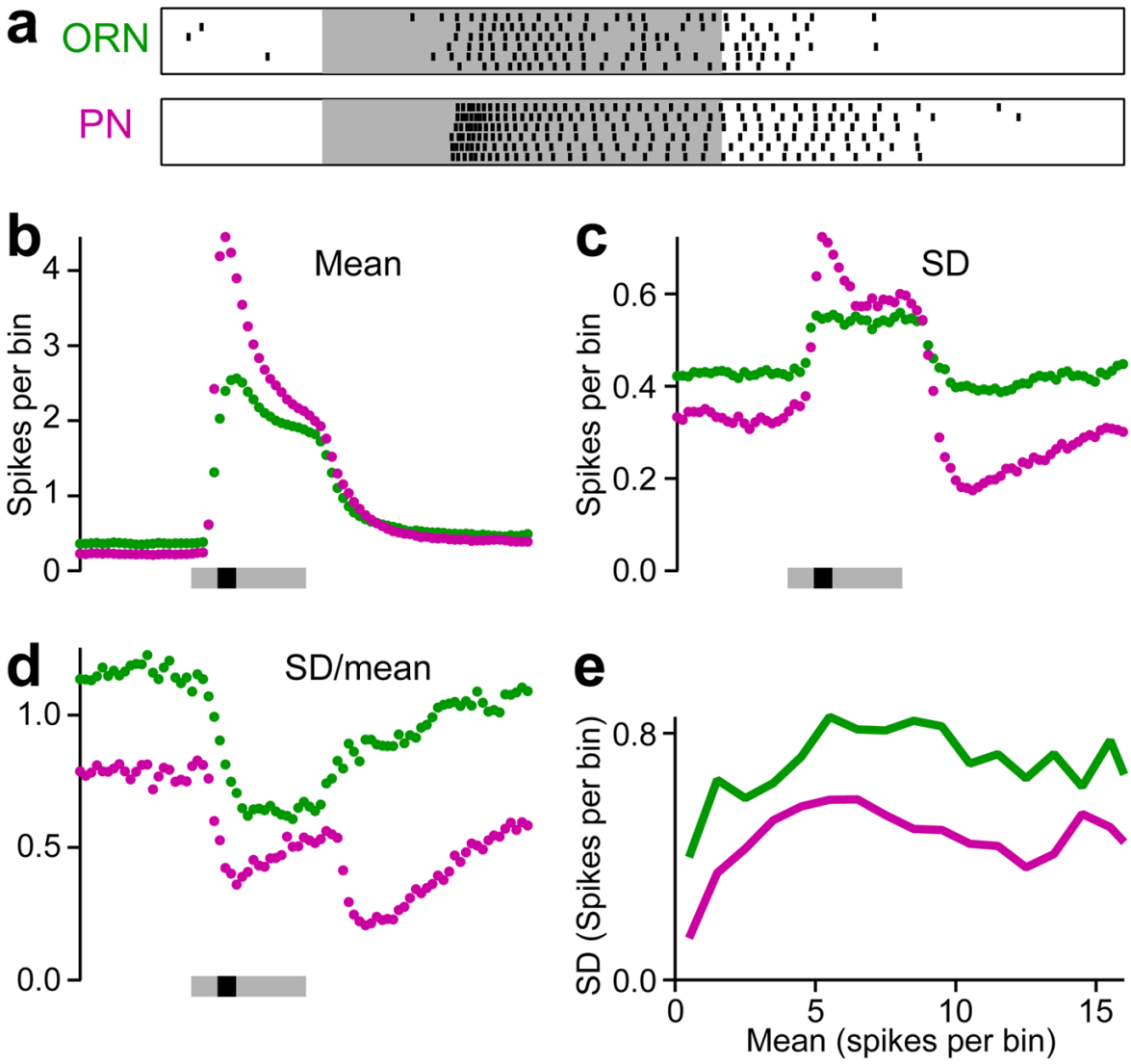


**Figure 1. Odor responses are more reliable in PNs than in ORNs**

(a) An ORN and a PN corresponding to the same glomerulus (VA2) responding to the same odor (geranyl acetate). Each tick represents a spike, and each row in a raster represents a different trial. Gray bar is 500-ms odor stimulus period.

(b) Mean odor responses are larger in PNs (magenta) than in ORNs (green). Spikes were counted in 50-ms bins and averaged across 5 trials with the same odor, then averaged across all blocks of trials (all odors and all experiments). Gray bar is stimulus period, black bar is 100-ms period when average PN firing rates are maximal.

(c) SD of spike counts in 5 trials with the same odor, averaged across all blocks of trials (all odors and all experiments).

(d) Coefficient of variation (SD/mean) of spike counts in 5 trials with the same odor, averaged across all blocks of trials. Note that the CV of PN responses drops again after odor offset. This is because some responses contain zero spikes for an epoch following odor offset, and so the SD in these bins is zero for some responses.

(e) Average SD of spike counts is lower for PNs than for ORNs even when mean firing rates are matched. SDs were measured for all counting windows in all blocks of trials, binned

according to mean firing rate, and averaged across all counting windows in the same bin. Note that because SD depends sublinearly on mean, average CV is larger than (average SD)/(average mean).

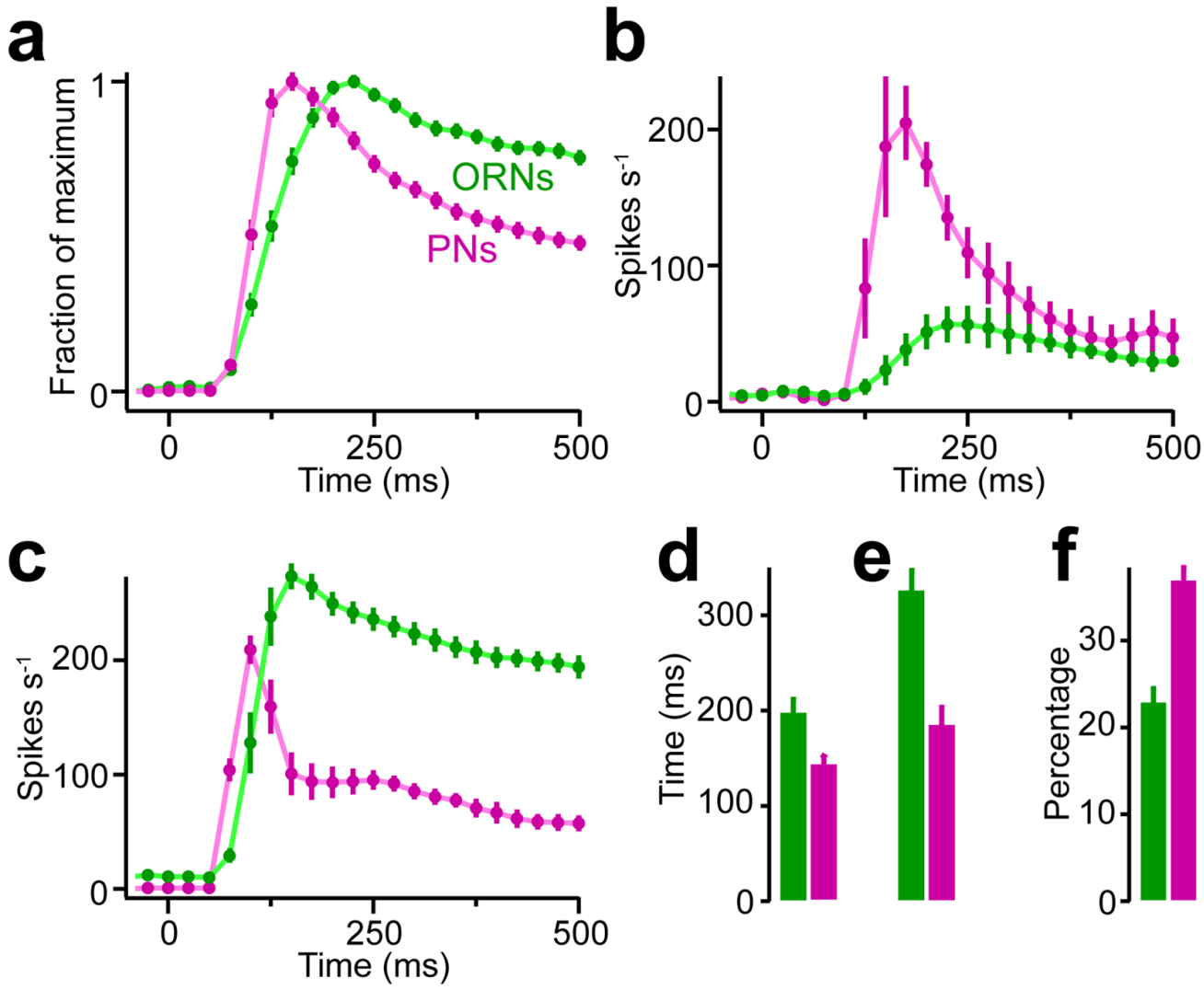


**Figure 2. PNs preferentially transmit the rising phase of ORN signals**

(a) Average peak-normalized peri-stimulus time histograms (PSTHs), averaged across all odors and all glomeruli (± s.e.m.). Note that PN responses rise and decay more rapidly than ORN responses. Odor stimulation begins at 0 ms and ends at 500 ms.

(b) An example comparing the responses of pre- and postsynaptic neurons to the same odor. PSTHs show the average response of ORNs and PNs in glomerulus VA2 to geranyl acetate (mean ± s.e.m., averaged across experiments). Note that the PN response is robust at a time point when the ORNs have just begun to respond, and the PN response begins decaying before the ORNs have peaked.

(c) Another example: PSTHs for ORNs and PNs in glomerulus DM1 showing responses to ethyl butyrate. The PN response rises faster and peaks earlier, even though in this case the PN peak is smaller.

(d) Compared to ORN responses, PN responses have a shorter latency to reach 90% of the response peak (mean ± s.e.m. across all blocks of trials; see Supplementary Methods).

(e) PN responses have a faster decay from peak to half-peak.

(f) A larger percentage of the total spike count occurs in the first 200 ms after odor onset for PN responses as compared to ORN responses.

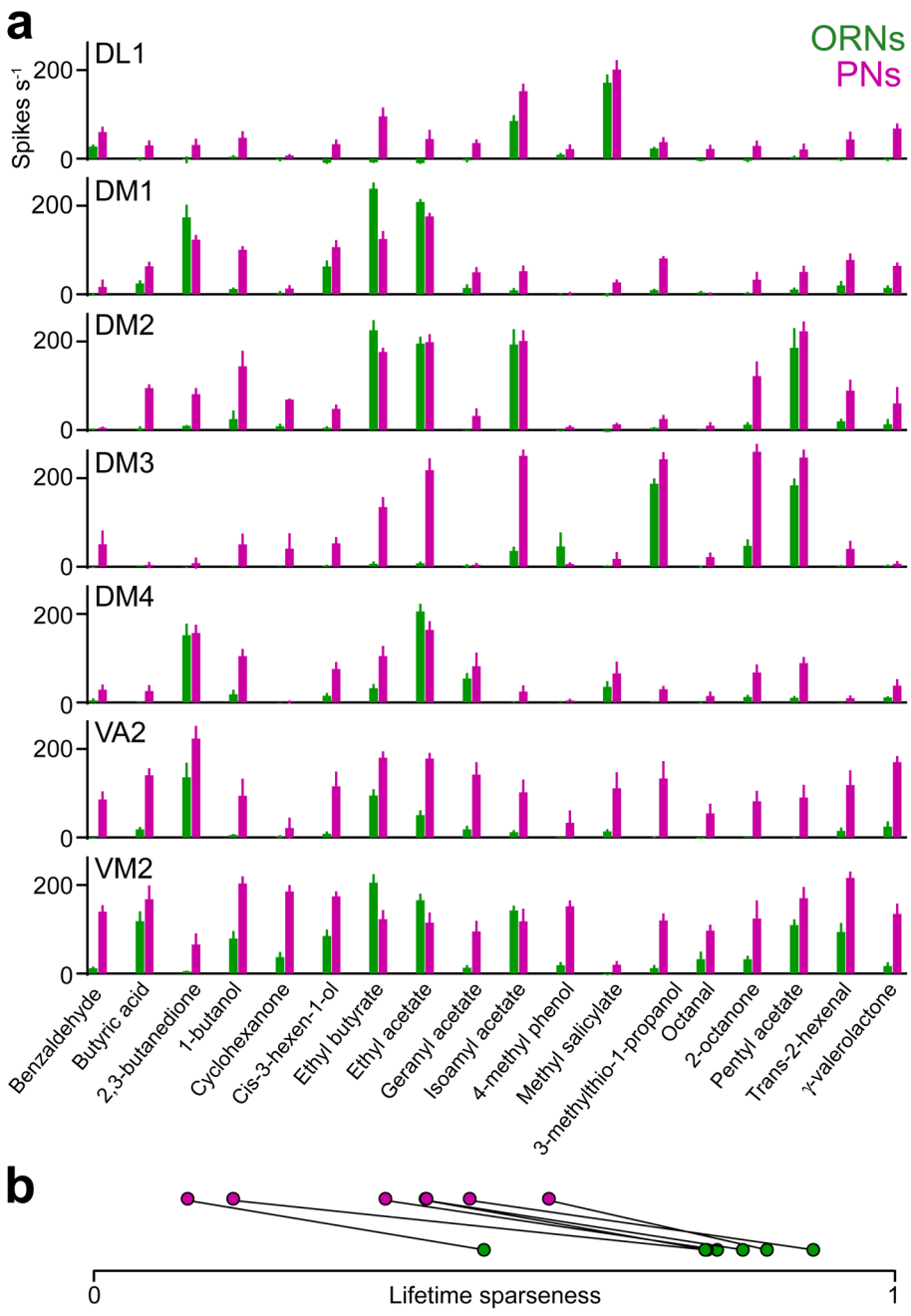


**Figure 3. ORNs and PNs differ in their odor selectivity**

(a) Response profiles for 7 ORN types (green) and 7 PN types (magenta) corresponding to the same glomeruli. Bars show averages across all experiments (± s.e.m., see Supplementary Table 2 for *n*). Responses are measured as the mean spike rate during the 100-ms epoch when firing rates are peaking (black bar in Fig. 1b-d), minus baseline firing rate. Results are similar over the entire 500-ms stimulus period (Supplementary Fig. 3).

(b) The selectivity of each response profile is quantified as lifetime sparseness[48, 29] (see Supplementary Methods; 0 = non-selective, 1 = maximally selective). ORNs and PNs corresponding to the same glomeruli are connected. PNs are consistently less selective than

their corresponding ORNs. The highest ORN sparseness value is for glomerulus DL1, and the lowest is for glomerulus VM2.

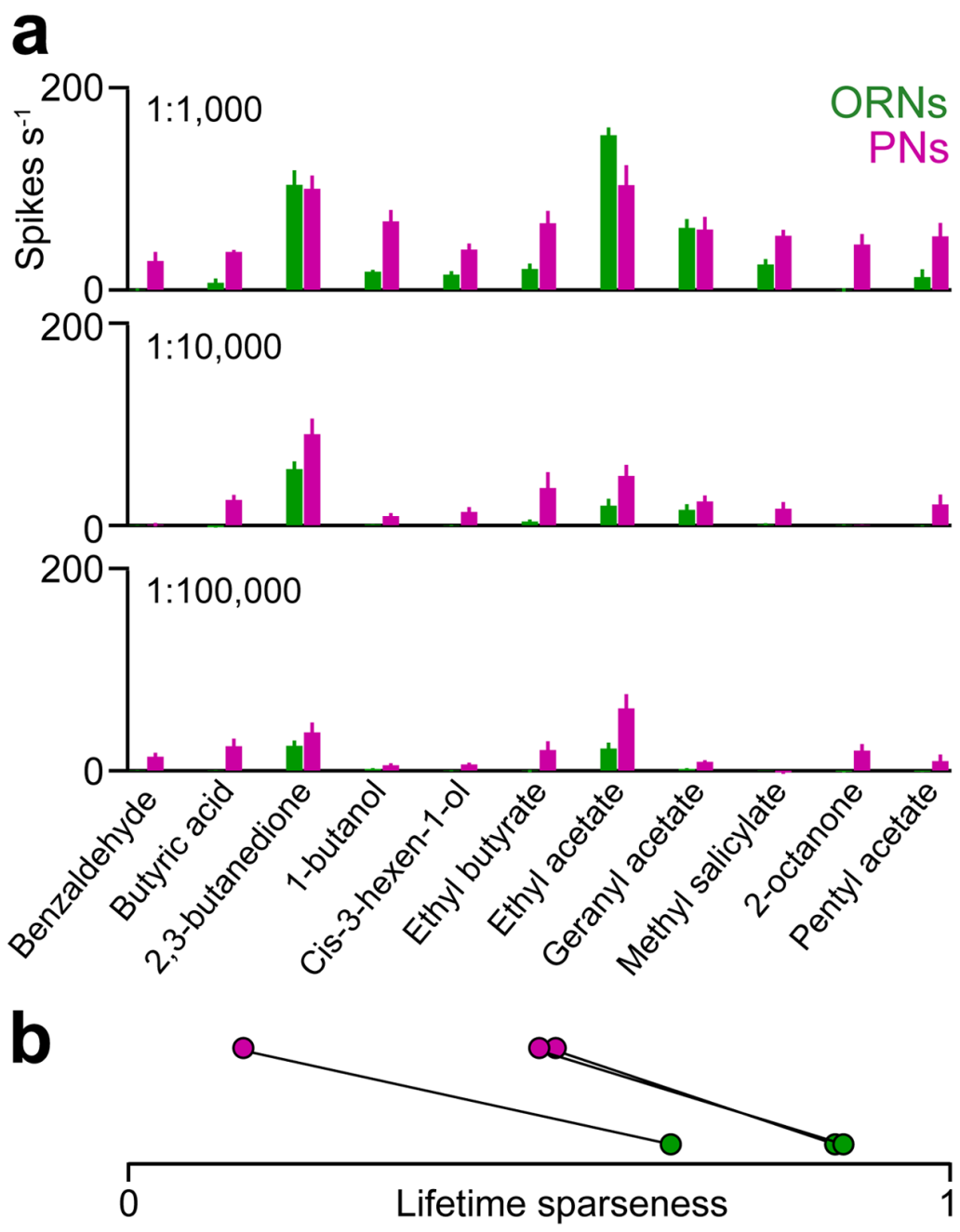


**Figure 4. ORNs and PNs differ in their odor selectivity even at low stimulus intensities**

(a) Response profiles for DM4 ORNs and PNs to a panel of 11 odors at 3 different concentrations. Bars show averages across all experiments (± s.e.m., see Supplementary Table 3 for *n*). Because the response peak tended to occur later for more dilute stimuli, we here measured responses as mean spike rate during the entire 500-ms stimulus period, minus baseline firing rate (as in Supplementary Fig. 3).

(b) The selectivity of each response profile for the 3 different odor dilutions. ORNs and PNs corresponding to the same dilution are connected. Note that DM4 PNs are consistently less selective than DM4 ORNs at all three concentrations. (Selectivity at the 1:1000 dilution is

slightly different than the selectivity value plotted in Supplementary Fig. 3 for this glomerulus because here we used only a subset of our 18 test odors.)

**a**

| Mean rate ± S.D. (spikes $s^{-1}$) | | ( Sample rate *Sample rank* ) | | | | | | | |
|---|---|---|---|---|---|---|---|---|---|
| ORN | PN | ORN sample 1 | | ORN sample 2 | | PN sample 1 | | PN sample 2 | |
| 4.3 ± 13.9 | 28.7 ± 36.1 | –20.0 | *18* | 14.3 | *9* | –34.5 | *18* | 86.2 | *7* |
| 1.5 ± 4.0 | 25.3 ± 41.1 | 6.0 | *10* | 6.3 | *11* | –6.2 | *16* | –3.5 | *18* |
| 152.1 ± 86.6 | 156.9 ± 62.5 | 66.3 | *3* | 317.4 | *1* | 152.0 | *3* | 111.2 | *4* |
| 18.2 ± 31.1 | 104.5 ± 54.8 | 15.4 | *7* | 39.1 | *5* | 78.5 | *7* | 103.1 | *5* |
| –0.5 ± 2.0 | 0.65 ± 7.1 | –1.3 | *14* | –7.6 | *12* | 4.1 | *15* | –2.5 | *17* |
| 14.6 ± 21.8 | 75.5 ± 50.1 | –17.9 | *17* | 44.3 | *18* | 90.6 | *6* | 159.1 | *1* |
| ⋮ | ⋮ | ⋮ | | ⋮ | | ⋮ | | ⋮ | |
| etc. | | | | | | | | | |

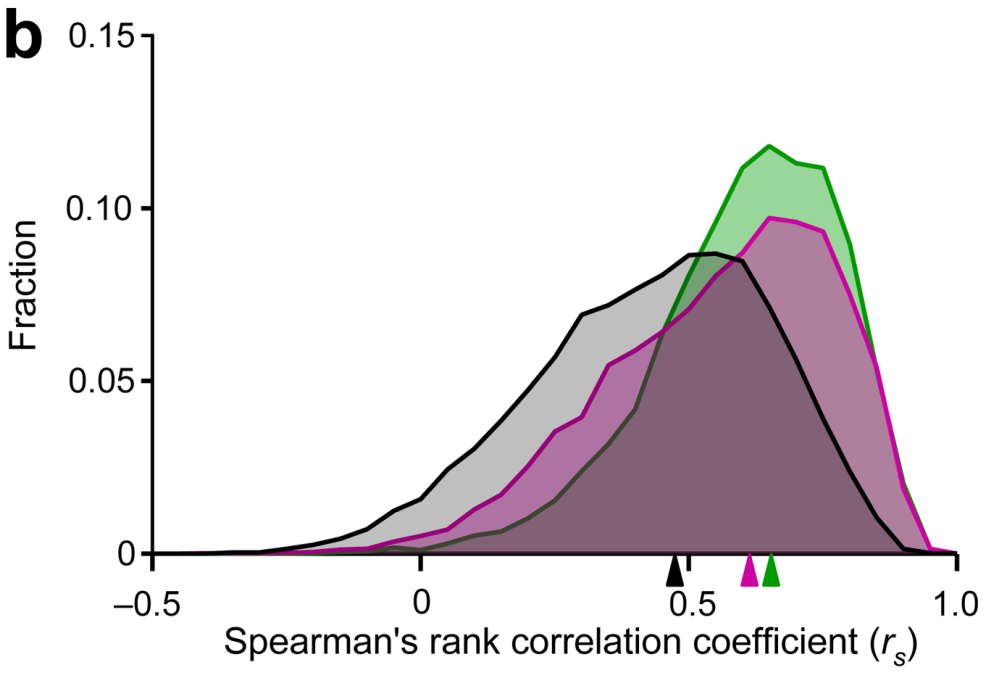


**Figure 5. The rank order of ORN and PN odor preferences is different**

(a) An example illustrating how we computed correlations between the odor ranks of individual cell response profiles. Here we show the mean and SD of the ORN and PN response profiles for glomerulus DM4. (Note the table is truncated after 6 odors.) We drew randomly from these distributions to produce representative simulated profiles for 2 individual ORNs and 2 individual PNs (arrows). Next we ranked the odors in each individual response profile (blue). In this example, the correlation coefficient between the 18 odor ranks of ORN sample 1 and ORN sample 2 ($r_s$) is 0.79. Correlation coefficients are somewhat lower for PN/PN comparisons (0.58 in this example). By comparison with either of these, ORN/PN correlations are much lower (0.33, 0.39, 0.42, and 0.46 in this particular example).

(b) Histograms showing the distribution of Spearman's rank correlation coefficients ($r_s$), accumulated across 2000 runs of the simulation procedure for each glomerulus. Arrowheads indicate median of each distribution. The ORN/PN correlations (gray) do not lie between the ORN/ORN (green) and PN/PN (magenta) correlations, indicating that ORN and PN odor ranks are not drawn from the same underlying mean distribution.

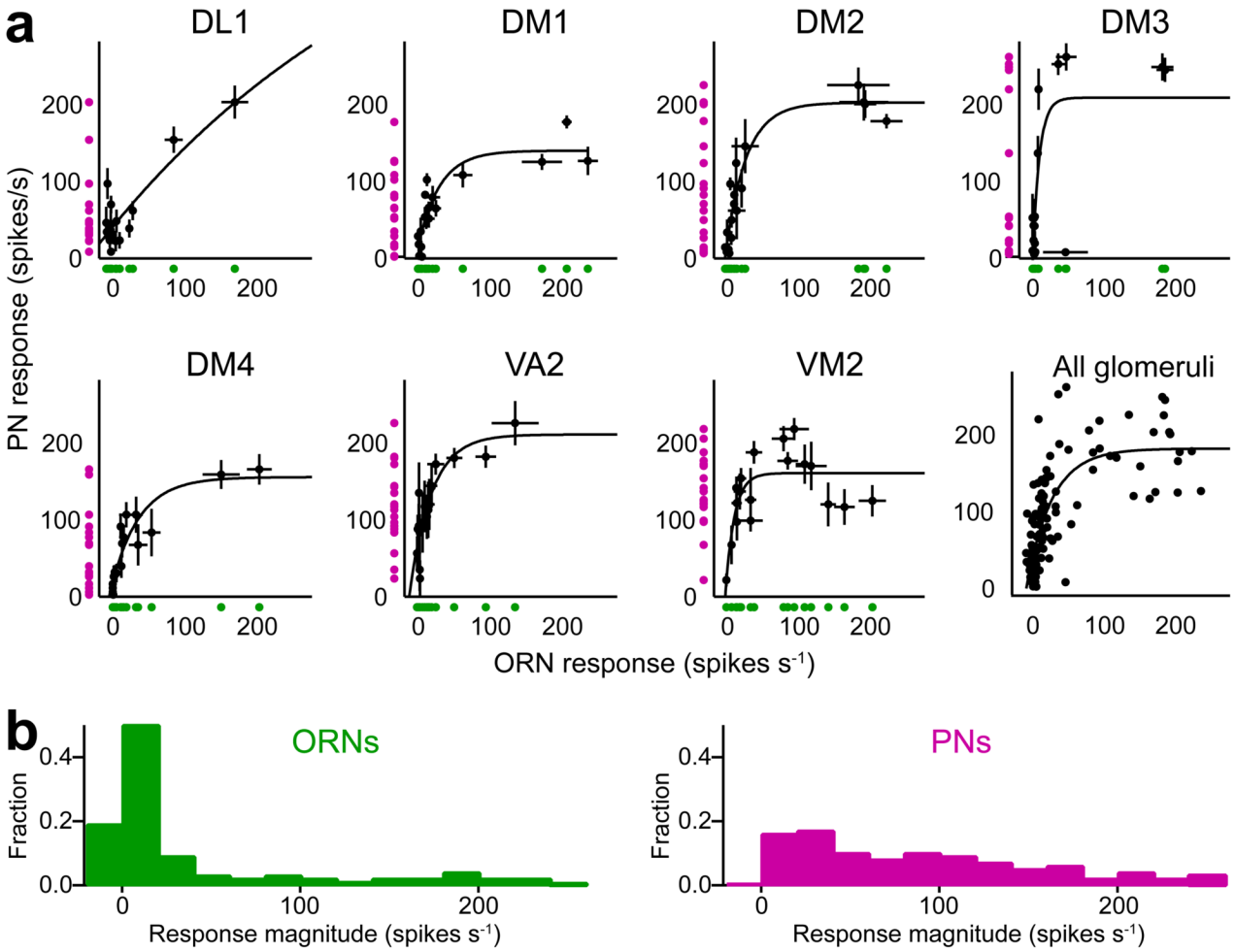


**Figure 6. PN odor responses are partly explained by a highly nonlinear transformation of their direct ORN inputs**

(a) For each glomerulus, average PN response to an odor is plotted versus the average ORN response to that odor (black symbols, ± s.e.m.). Curves are exponential fits ($y=y_0+A\cdot e^{kx}$). Green and magenta symbols are projections of the data onto the *x*- and *y*-axes, showing that odor responses generally occupy a PN's dynamic range more evenly than they occupy an ORN's dynamic range. Responses are measured as the mean spike rate during the 100-ms epoch when firing rates are peaking (with no baseline subtraction), but results are similar if responses are measured as the mean spike rate during the entire 500-ms stimulus period (see Supplementary Fig. 5).

(b) Histograms of ORN and PN response magnitudes. Each histogram is accumulated across all 126 response magnitudes (= 7 glomeruli ×18 odors). The PN histogram is flatter than the ORN histogram, indicating that PNs use their dynamic range more efficiently.

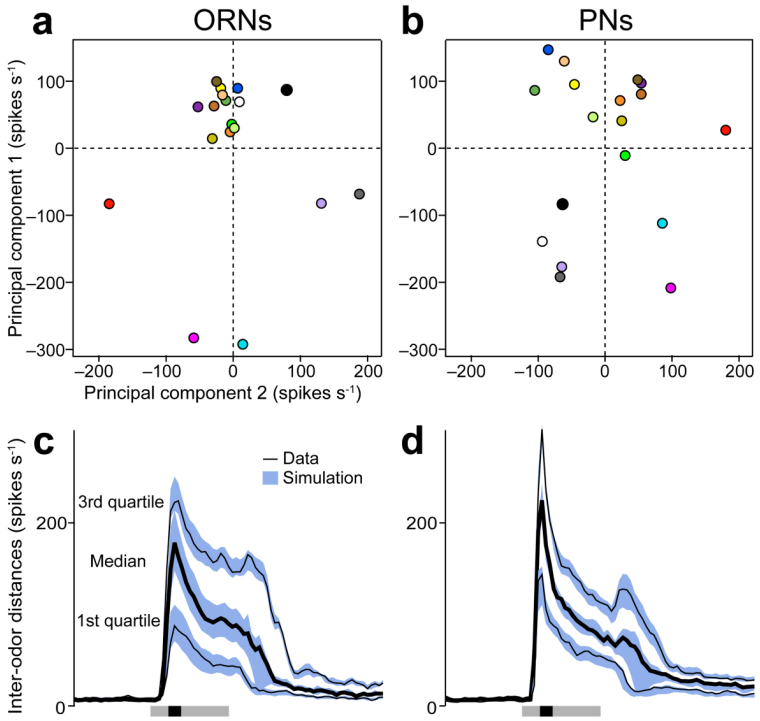


**Figure 7. Odors are distributed more uniformly in ensemble PN coding space than in ensemble ORN coding space**

(a) Average odor responses from 7 ORN types projected onto the space defined by the first two principal components. Each point represents a different odor.

(b) Same as (a) for PN data (with the same color conventions), showing a more uniform separation between odor representations.

(c) The difference between ensemble ORN responses to different odors is quantified as the Euclidean distance between odor representations in 7-dimensional space. Distances are computed for all 153 pairwise combinations of the 18 odor stimuli, and the median and interquartile range of this distribution are plotted here for each time point. The wide interquartile range means that some odors are well-separated in ORN space, but many are very poorly separated. Blue bands indicate the range of results obtained by shuffling odor labels on each glomerular response profile (see Supplementary Methods).

(d) Same as (c) for PN responses. At the peak of the response (black bar), distances are significantly larger in PN space as compared to ORN space. PN responses then quickly accommodate (see Fig. 2), and so inter-odor distances shrink. However, the interquartile range of distances remains smaller than in ORN space. This indicates a more uniform distribution of distances. As in (c), shuffling odor labels on each glomerular response profile produces a range of results (blue bands) that resembles the real data.

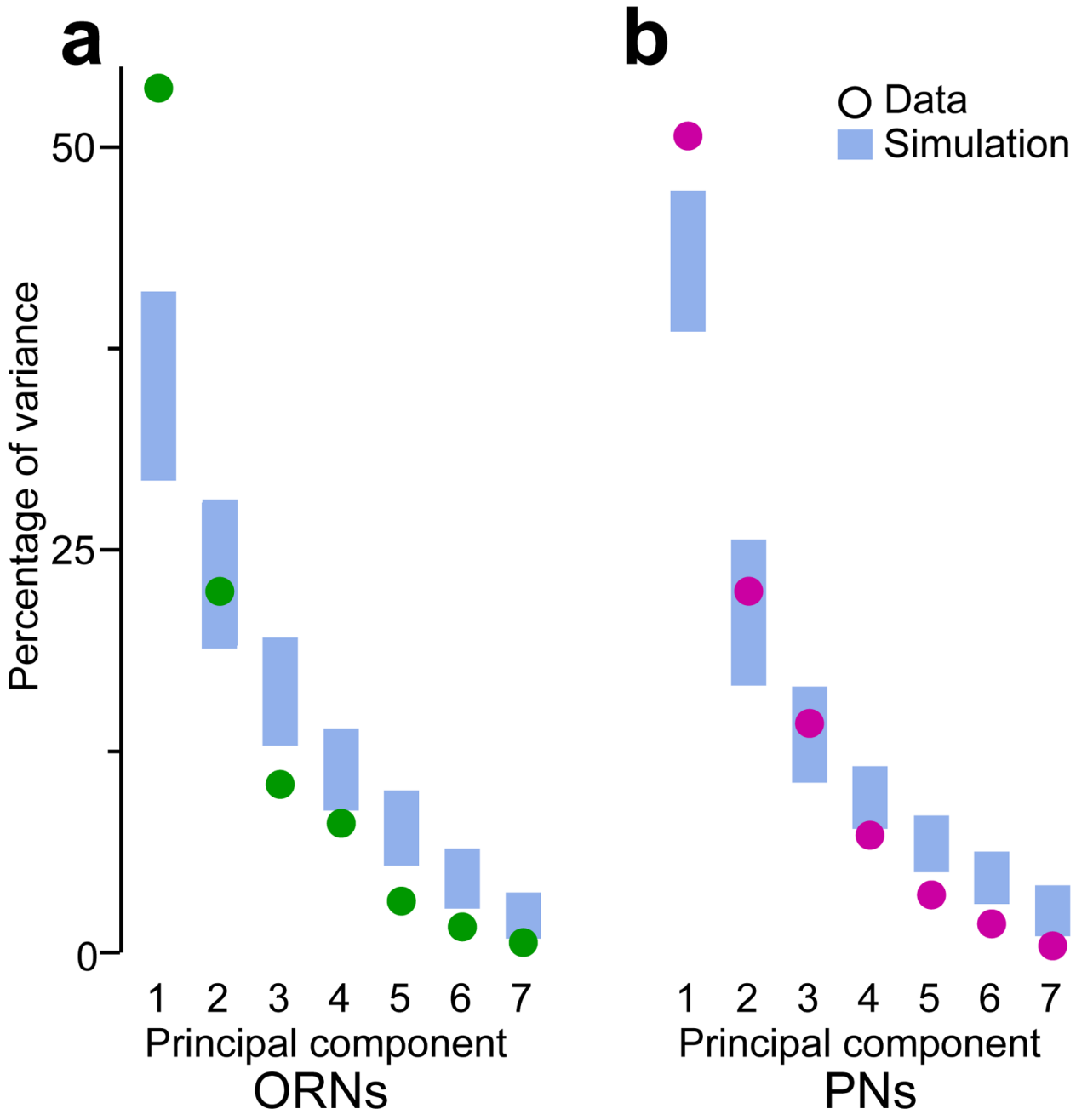


**Figure 8. Correlations between different glomeruli are similar for ORNs and PNs**

(a) Principal components analysis (PCA) was applied to the 18×7 ORN response matrix. The magnitude of the variance accounted for by each PC (green circles) is a measure of the correlations between different ORN types. Blue bands indicate the range of results obtained by shuffling odor labels on each glomerular response profile (see Supplementary Methods). Comparison between data and simulation shows that ORNs are less independent in their odor responses than we would expect based simply on the distribution of response magnitudes within each glomerular coding channel.

(b) Same as (a) for the 18×7 PN response matrix. Correlations between PN types are similar to correlations between ORN types.

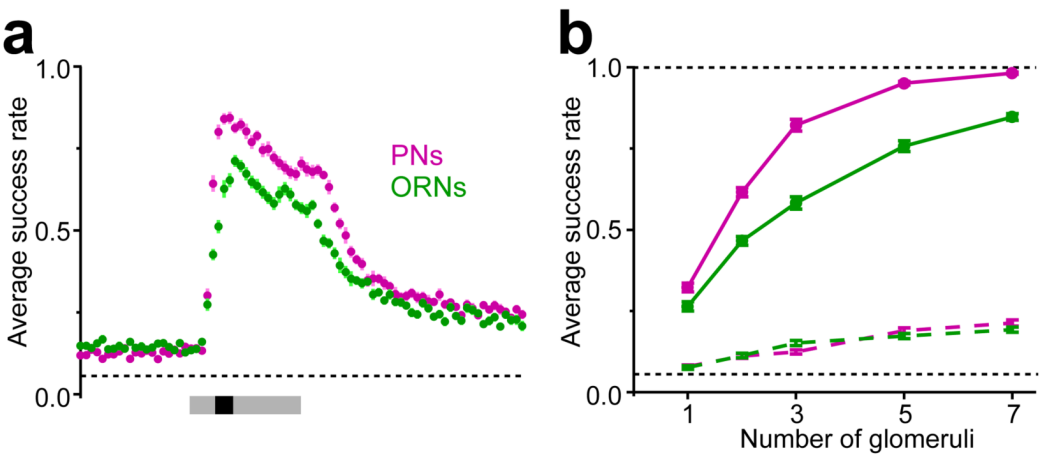


**Figure 9. A linear discriminator can classify odors more accurately with responses from multiple PNs than with responses from the same number of ORNs**

(a) LDA odor classification success rate with data sets that include cells from 3 glomerular classes. All possible combinations of three glomeruli were sampled. Points are mean ± s.e.m., averaged across 20 runs of the classification procedure. Dotted line is chance performance. (b) Success rate is higher for PN data than for ORN data, regardless of how many glomerular classes are included in the data set. Points are mean ± s.e.m., averaged over the 100-ms window shown in (a), and then averaged across 20 runs of the classification procedure. Dashed green and magenta lines plot the classification success rate during the baseline period prior to odor onset; this is an artifact of varying spontaneous activity rates (see text), and ORN and PN performance is similar. Dotted black lines indicate perfect and chance performance.